Structure and absolute configuration of toxic polyketide pigments from the fruiting bodies of the fungus *Cortinarius rufo-olivaceus*†

Jin-Ming Gao,*[a] Jian-Chun Qin,[b,c] Gennaro Pescitelli,[d] Sebastiano Di Pietro,[d] Ya-Tuan Ma[a] and An-Ling Zhang[a]

Received 12th February 2010, Accepted 14th May 2010
First published as an Advance Article on the web 9th June 2010
DOI: 10.1039/c002773a

Two new polyketide-derived pigments, named rufoolivacins B (**2**), and D (**4**), with a 4′,10-coupled aryl linkage between polysubstituted 1-naphthol and 1,4- or 1,2-anthraquinone, together with nine known metabolites including rufoolivacins A (**1**) and C (**3**), have been isolated from the fruiting bodies of the Chinese toadstool *Cortinarius rufo-olivaceus* (basidiomycetes). Their structures were characterized on the basis of spectroscopic methods, including 2D-NMR experiments (COSY, NOESY, HSQC, and HMBC). The axial chirality of **1** and **2** was assigned through analysis of their CD spectra and ZINDO and TDDFT calculations. Compounds **3** and **4** were found to be unusual natural products incorporating an *ortho*-anthraquinone chromophore. All the metabolites were shown to be toxic toward the brine shrimp.

Introduction

Fungal polyketides constitute a large family of secondary metabolites endowed with a high degree of structural diversity and various biological activities.[1] Structurally complex and stereochemically challenging octaketides with a biaryl skeleton occur in various species of medicinal plants and fungi.[2,3] Usually, only a single stereoisomer is observed for a certain species, even in the presence of multiple chirality elements.

Pigments manufactured by those fungi that produce conspicuous fruit bodies (Macromycetes or Macrofungi) include a variety of natural products derived from the various biogenetic pathways. Among them, the polyketide anthraquinone pigments from the acetate–malonate pathway represent an important family of dyes that possess biological activities and are used in medicine and food processing. To date, a large number of fungal pigments have been found to be generated by the macromycetes, genera *Cortinarius* and *Dermocybe*, belonging to the family Cortinariaceae.[4,5,6,7] According to the position of the C–C bond formed during the oxidative coupling of the putative precursors atrochrysone or torosachrysone, dimeric pre-anthraquinones can be classified as belonging to the (7-10′)-phlegmacin, (5-5′)-atrovirin, or (7-7′)-flavomannin groups.[8,9] In contrast, there is a small rare family of natural pigments, belonging to the rufoolivacin type, which are composed of an oxidized naphthalene-derived tarachrysone monomethyl ether unit linked to a pre-anthraquinone moiety *via* 4′-10 C–C oxidative phenolic coupling.

The edible mushroom *Cortinarius rufo-olivaceus* (Pers.) Fr. is mainly distributed in China and Europe, in particular, in the Ningxia and Mongolia provinces of China, and enjoys extremely high popular reputation for its health benefits.[10,11] However, the chemical constituents of this species have not been thoroughly studied.

In the course of our ongoing search for biologically active substances from higher fungi (Macromycetes),[12] we isolated and identified two new unique naphthalene–anthraquinone biaryls, rufoolivacin B (**2**) and rufoolivacin D (**4**) (Chart 1) together with nine known polyketides, rufoolivacin A (**1**),[8] rufoolivacin C (**3**),[13] (3*S*)-torosachrysone-8-*O*-methyl ether (**5**),[14] physcion (**6**),[11] 1-hydroxy-6,8-dimethoxy-3-methylanthraquinone (**7**),[15] torachrysone-8-*O*-methyl ether (**8**),[16] citreorosein 6,8-dimethyl ether (**9**),[8] sinapiquinone (**10**),[17] and anhydroflavomannin-9,10-quinone 6,6′,8′-tri-*O*-methyl ether (**11**)[18] (Chart 1 and 2), from the fruiting bodies of the higher basidiomycete *C. rufo-olivaceus*. In the present study, we report the isolation and structure elucidation of these new metabolites, as well as their toxic activity against the brine shrimp. In addition, the configurations of rufoolivacins A (**1**) and B (**2**) have been established in this work for the first time by analysis of their circular dichroism (CD) spectra and by using quantum-mechanics CD calculations.

Results and discussion

The AcOEt-soluble portion of the MeOH extract (187 g) of the dried fruiting bodies of *C. rufo-olivaceus* was fractionated by normal and reverse phase column chromatography and preparative TLC, followed by purification over Sephadex LH-20 column to afford 11 compounds **1–11**, including two novel metabolites **2** and **4**.

[a]*Natural Medicinal Chemistry Research Centre, College of Science, Northwest A & F University, Yangling, Shaanxi, 712100, People's Republic of China. E-mail: jinminggaocn@yahoo.com.cn*
[b]*College of Plant Science, Jilin University, Changchun 130062, People's Republic of China*
[c]*Department of Organic Chemistry, University of Göttingen, Tammannstrasse 2, D-37077, Göttingen, Germany*
[d]*Università di Pisa, Dipartimento di Chimica e Chimica Industriale, Via Risorgimento 35, 56126, Pisa, Italy*

† Electronic supplementary information (ESI) available: : DFT-calculated structures of (a*S*)-**1**; CD spectra of rufoolivacins **A**–**D** in CH_3CN and THF; comparison between CAM-B3LYP/SVP and CAM-B3LYP/TZVP calculations; ZINDO/S-CI calculations. See DOI: 10.1039/c002773a

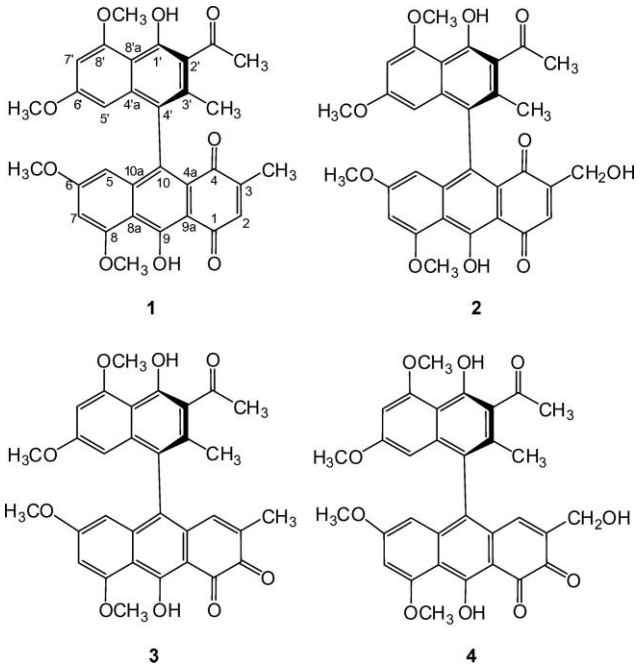

Chart 1

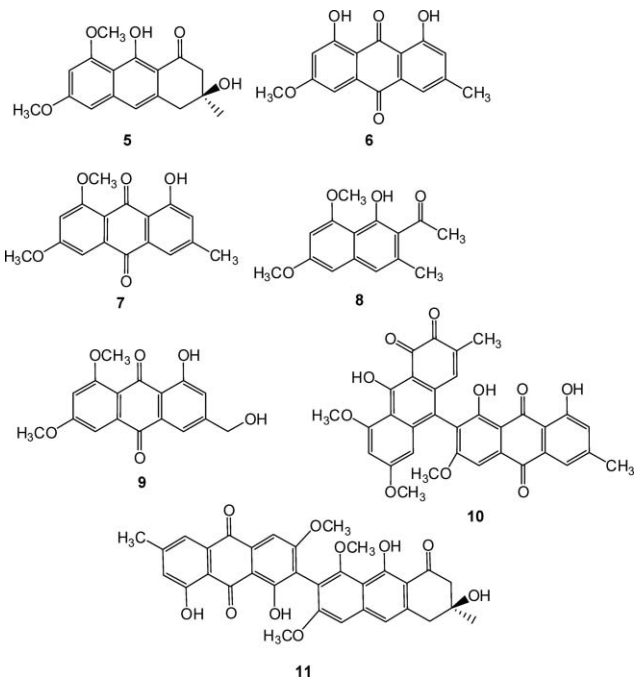

Chart 2

Two known pigments were characterized as rufoolivacins A (**1**) and C (**3**) on the basis of positive-ion high-resolution ESI-MS, UV, IR and 1D and 2D NMR spectra (Tables 1 and 2) and by comparison of their spectroscopic data with the literature values.[8,13,19,20] However, the absolute stereochemistry (axial chirality) of **1** and **3** had not been previously determined. Moreover, although compound **3** had been previously isolated from the European toadstool *C. rufo-olivaceus*, NMR spectral data of **3** were not reported.[13]

Table 1 ^{1}H- (600 MHz) and ^{13}C-NMR (150 MHz) spectroscopic data (ppm) of compounds **1** and **2** in acetone-d_6[a]

	1		**2**	
position	δ_C	δ_H (mult, J in Hz)	δ_C	δ_H (mult, J in Hz)
1	178.7 s		178.8 s	
2-CH	137.9 d	6.81 q, (1.5)	135.4 d	7.05 dd, (1.8/1.8)
3	137.8 s		141.4 s	
3-CH_3	16.1 q	1.79 s		
3-CH_2	—		58.9 t	4.30 br s
4	182.7 s		181.8 s	
4a	142.8 s		142.9 s	
5-CH	104.5 d	6.09 d, (2.3)	104.7 d	6.10 d, (2.3)
6	165.8 s		165.8 s	
6-OCH_3	55.6 q	3.65 s	55.9 s	3.66 s
7-CH	99.7 d	6.76 d, (2.3)	99.8 d	6.77 d, (2.3)
8	164.5 s		164.5 s	
8-OCH_3	56.7 q	4.05 s	56.8 q	4.06 s
8a	133.1 s		133.9 s	
9	174.9 s		175.0 s	
9-OH		16.1 s		16.2 s
9a	110.3 s		110.1 s	
10	111.5 s		111.6 s	
10a	130.5 s		130.3 s	
1′	153.2 s		153.2 s	
1′-OH		9.89 s		9.90 s
2′	124.6 s		124.6 s	
2′-$COCH_3$	204.7 s		204.7 s	
2′-$COCH_3$	32.5 q	2.58 s	32.6 q	2.58 s
3′	135.2 s		135.1 s	
3′-CH_3	17.6 q	1.92 s	17.7 q	1.93 s
4′	123.8 s		123.3 s	
4′a	137.6 s		137.9 s	
5′-CH	99.2 d	6.18 d, (2.3)	99.3 d	6.18 d, (2.3)
6′	160.4 s		160.4 s	
6′-OCH_3	55.6 q	3.53 s	55.6 q	3.52 s
7′ -CH	98.4 d	6.66 d, (2.2)	98.4 d	6.65 d, (2.2)
8′	159.0 s		159.1 s	
8′-OCH_3	57.2 q	4.20 s	57.2 q	4.20 s
8′a	109.8 s		109.7 s	

[a] Assigned by COSY, HSQC, NOESY, and HMBC experiments. The multiplicity was measured in the DEPT experiment.

Rufoolivacin B (**2**) was obtained as an optically active red amorphous powder with a melting point of 342–346 °C. The molecular formula was determined to be $C_{32}H_{28}O_{10}$ by positive high-resolution ESI-MS (*m/z*: 573.1748[M+H]$^+$, calcd. for $C_{32}H_{29}O_{10}$ 573.1755), in conjunction with NMR spectroscopy (Table 1) which indicated 18 degrees of unsaturation. The UV absorption bands (λ_{max} 237, 286, 325, and 512 nm) and IR spectra (ν_{max} 3422, 1618 (conjugated carbonyl), and 1599 cm^{-1}) of **2** are very similar to the corresponding data for **1**.

Comparison of the ^{1}H and ^{13}C NMR data (Table 1) of **2** with those of **1** and **8** showed the presence of a substructure similar to that of **1** (indicated as **a**, Fig. 1). The other moiety (**b**, Fig. 1) contained a doubly chelated phenolic hydroxyl resonating at δ 16.2 (s, 9-OH), suggesting the formation of an intramolecular hydrogen bond between the hydroxyl and a C-8 methoxy (δ 4.06) or a carbonyl carbon C-1 (δ 178.8). The ^{1}H-NMR spectrum showed two aromatic proton signals at δ 6.10 (d, H-5) and 6.77 (d, H-7) with a *meta*-coupling constant (J = 2.3 Hz) along with another C-6 methoxy (δ 3.66), a hydroxyl methyl at δ 4.30 (br s) and one quinoid proton at δ 7.05 (d, J = 1.8 Hz, H-2). The above data indicated the molecule possessed a 6,8-dimethoxy-9-hydroxyl-1,4-anthraquinone unit. This substructure was further supported by

Table 2 ^{1}H- (600 MHz) and ^{13}C-NMR (150 MHz) spectroscopic data (ppm) of compounds **3** and **4** in acetone-d_6[a]

	3		**4**	
position	δ_C	δ_H (mult, J Hz^{-1})	δ_C	δ_H (mult, J Hz^{-1})
1	189.7 s		189.7 s	
2	184.9 s		184.2 s	
3	136.4 s		137.1 s	
3-CH_3	16.5 q	1.90 s		
3-CH_2			59.1 t	4.38 br s
4	133.0 d	6.92 d, J = 1.0	133.5 d	7.04 dd, J = 1.75, 1.75
4a	142.1 s		153.9 s	
5-CH	102.7 d	5.97 d, J = 2.19	102.8 d	5.98 d, J = 2.1
6	164.0 s		164.1 s	
6-OCH_3	55.6 q	3.42 s	55.7 q	3.43 s
7-CH	100.9 d	6.81 d, J = 2.3	101.0 d	6.83 d, J = 2.4
8	163.2 s		163.3 s	
8-OCH_3	56.7 q	4.04 s	56.7 q	4.04 s
8a	114.0 s		114.1 s	
9	167.0 s		167.4 s	
9-OH		15.81 s		15.86 s
9a	109.0 s		108.8 s	
10	132.6 s		132.6 s	
10a	127.8 s		127.9 s	
1′	152.0 s		152.1 s	
1′-OH		9.76 s		9.76s
2′	125.0 s		125.0 s	
2′-$COCH_3$	204.9 s		204.8 s	
2′-$COCH_3$	32.7 q	2.57 s	32.7 q	2.57 s
3′	134.6 s		133.0 s	
3′-CH_3	17.3 q	1.76 s	17.2 q	1.75 s
4′	127.3 s		127.1 s	
4′a	137.7 s		138.0 s	
5′-CH	97.9 d	6.23 d, J = 2.34	98.3 d	6.24 d, J = 2.4
6′	159.0 s		159.8 s	
6′-OCH_3	55.4 q	3.57 s	55.4 q	3.58 s
7′-CH	98.3 d	6.58 d, J = 2.18	98.0 d	6.59 d, J = 2.1
8′	159.8 s		159.0 s	
8′-OCH_3	57.0 q	4.17 s	57.0 q	4.17 s
8′a	110.2 s		110.0 s	

[a] Assigned by COSY, HSQC, NOESY, and HMBC experiments. The multiplicity was measured in the DEPT experiment.

the key HMBC correlations (Fig. 1) of H-5 and C-7, C-8a, and C-10; H-7 and C-5, C-6, C-8, and C-8a; H-2 and CH_2-3, C-4, C-9a; and CH_2 and C-2, C-3, and C-4. The absence of a low-field signal attributable to H-10 (*ca.* δ 8) for the 1,4-anthraquinone moiety helped establish that the naphthol moiety (**a**) is linked to C-10 position of the 1,4-anthraquinone (**b**) unit.[21] Besides, the appearance of the H-2 doublet at δ 7.05 (J = 1.8 Hz) and the absence of the H-4′ singlet at *ca.* δ 7.3 for the naphthol moiety

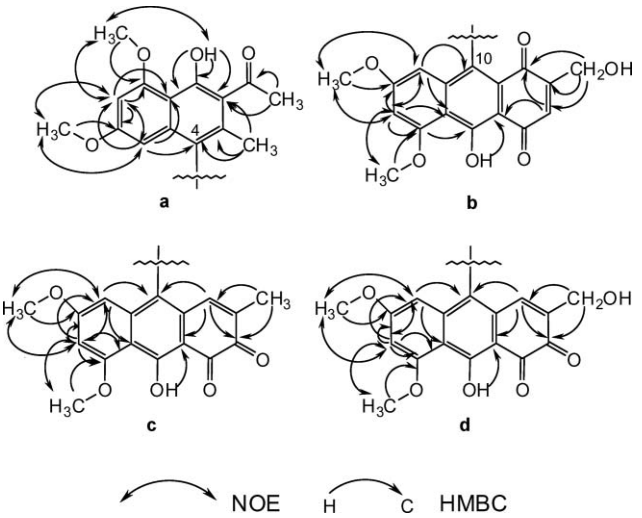

Fig. 1 Key HMBC and NOESY couplings in substructures **a–d** in natural pigments **1–4**. Substructure **a** is common for **1–4**, whereas **b** belongs to **2**, **c** to **3** and **d** to **4**.

suggested that the 1,4-anthraquinone moiety is coupled to the C-4′ position of the naphthalene skeleton.[16,21]

The ^{13}C-NMR (Table 1) data of compound **2** were almost identical to those reported in the literature for rufoolivacin A (**1**)[8] as well as to those obtained on our sample of **1**. The only difference was that the C-3-linked methyl in the quinone nucleus at δ 16.1 in **1** was replaced by one oxygen-bearing methylene at δ 58.9, and this indicated that **2** was a hydroxylated derivative of **1**. Thus, compound **2** was also a conjugate of 1-naphthol (**a**) and 1,4-anthraquinone (**b**) units *via* a 10-4′ aryl linkage. The structure of the new natural product **2** was determined to be 9-hydroxy-6,8-dimethoxy-3-hydroxylmethyl-10-(6′,8′-dimethoxy-2′-acetyl-3′-methyl-1′-hydroxynaphth-4′-yl)-1,4-anthraquinone, named rufoolivacin B (Chart 1).

Both compounds **1** and **2** may exist as tautomers relative to the hydrogen shift between oxygens attached at C-1 and C-9. One tautomer (Fig. 2, left) has a *p*-quinone-type structure and is labeled "PQ"; the second has naphthalene-1,5-dione-type structure (Fig. 2, right) and is labeled "ND". Apparently, "ND" type structures could be anticipated to be irrelevant, because of the loss of aromaticity in one ring. Rather surprisingly, however, ^{13}C-NMR spectra argued against this intuitive picture. In fact, the observed chemical shifts for C-1 and C-9 are very similar to each other (for **1**, 178.7 and 174.9 ppm, respectively; for **2**,

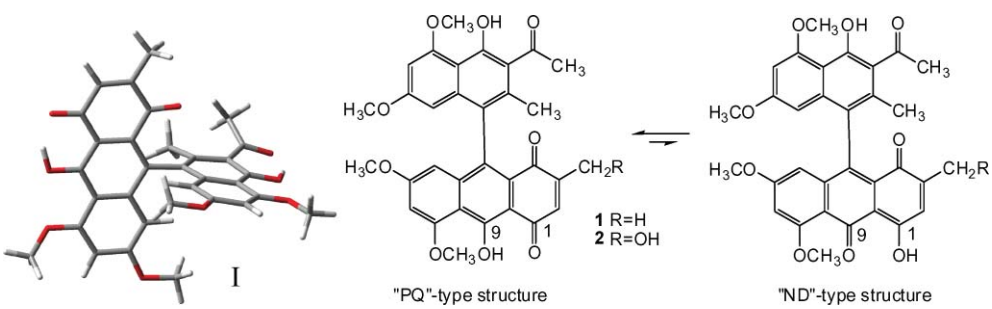

Fig. 2 Possible tautomeric form of compounds **1** and **2** and the lowest-energy DFT-optimized structure (I) for compound **1** (PQ tautomer).

178.8 and 175.0 ppm, respectively) and intermediate between the two values expected for a quinone and a phenol C-1 type carbon, as found respectively in the "PQ" and "ND" tautomers. Therefore, some incidence of "ND" structures was envisaged. However, molecular modeling calculations (see below) using DFT method revealed that structures for "ND" tautomers have substantially higher energy than the corresponding "PQ" tautomers. Therefore, the occurrence of the tautomerism was neglected in the following.

Rufoolivacin D (**4**) was obtained as red amorphous powder, with the molecular formula deduced as $C_{32}H_{28}O_{10}$ by positive high-resolution ESI-MS (*m/z*: 573.1754[M+H]$^+$, calcd. for $C_{32}H_{29}O_{10}$ 573.1755), in conjunction with NMR data (Table 2), indicating 18 degrees of unsaturation. The comparison of the ^{1}H- and ^{13}C-NMR data of **4** with those of **3** revealed that they share the same structural skeleton and substitution pattern. The obvious difference was that one of the two aromatic methyls at δ 16.5 and δ 1.90 ppm in **3** was replaced with a hydroxymethylene group (δ 59.1 and δ 4.38 ppm). This result was further supported by the analyses of the HMBC and NOESY correlations, as shown Fig. 1. The structure **4** of the new natural product was thus determined to be 9-hydroxy-6,8-dimethoxy-3-hydroxylmethyl-10-(6′,8′-dimethoxy-2′-acetyl-3′-methyl-1′-hydroxynaphth-4′yl)-1,2-anthraquinone, named rufoolivacin D (Chart 1). The complete assignment of all proton and carbon NMR signals was based on COSY, ROESY, HSQC, and HMQC experiments.

Rufoolivacins **1–4** are biaryls with hindered rotation around the biaryl axis and exist therefore as optically stable atropisomers. As expected, the natural samples in our hands were all optically active with $[\alpha]_D$ values between +88 and +320. To study the absolute stereochemistry (axial chirality) of compounds **1–4**, their UV/CD spectra were recorded in three different solvents (methanol, acetonitrile and THF).

The CD spectra of compounds **1** and **2** were very similar in the three solvents employed; those in methanol are shown in Fig. 3a, others in the Supporting Information†. They show a few moderately intense bands in the 200–350 nm region, followed by one or more weak bands at longer wavelengths. The two most intense signals appear as a positive CD couplet (*i.e.*, a positive CD band followed by a negative one at a shorter wavelength) centered around 250 nm, close to the absorption maximum observed at 237–238 nm in methanol. Thus, it was tempting to recognize for compounds **1** and **2** exciton-coupled CD spectra.[22] Application of the exciton-chirality method requires the chromophores and relative transitions giving rise to the observed couplet to be exactly identified. The most immediate treatment possible, which has been applied to structurally-related asperinines,[23] would identify compounds **1** and **2** as essentially 1,1′-binaphthyl derivatives, where the 1,1′ linkage corresponds to the C-4′/C-10 junction. If so, the positive couplet around 250 nm would be due to the exciton coupling between ^1B_b-type transitions, which are long-axis polarized in naphthalene ring.[24] The exciton chirality theory would then predict a positive couplet for a positive C-3′,C-4′,C-10,C-4a dihedral $\theta_{3'\text{-}4'\text{-}10\text{-}4a}$, corresponding for **1** and **2** to (a*R*) axial configuration (according to IUPAC nomenclature the group starting with C-4a′ has higher priority than that starting with C-3′). However, the aromatic rings in rufoolivacins are not simple naphthalenes, in particular, one ring is actually a 1,4-anthraquinone. Moreover, the middle of the 1,4-anthraquinone unit lies approximately along the direction of the chirality axis, and the most probable arrangement between the two rings is roughly perpendicular. In such circumstances, the exact "position" of the anthraquinone transition point-dipole should be known exactly to afford a safe configurational assignment *via* the exciton chirality method.[25] Only a rough procedure for determining the position of the transition point-dipole is available, but it is not applicable to the high-energy transitions of a complicate chromophore like 1,4-anthraquinone.

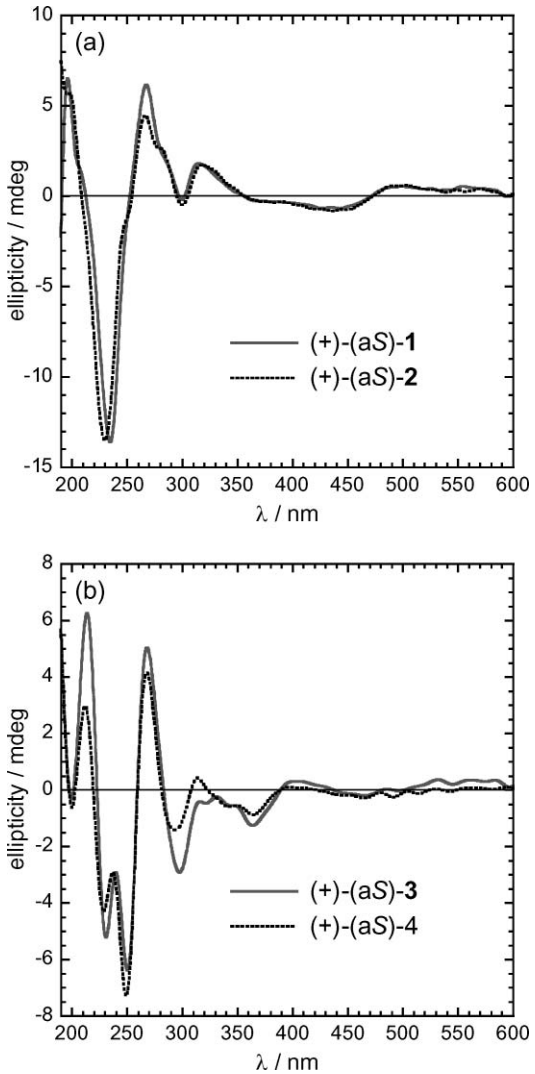

Fig. 3 CD spectra in methanol of rufoolivacins **1–4**. Conditions reported in the Experimental Section.

Therefore, we decided to run quantum-mechanical simulations of CD spectra to be compared with experimental ones.[26] In the present case, however, this procedure was also not free from difficulties, because of the molecular size and flexibility. As for the possible presence of tautomers, only the "PQ" tautomeric form was considered as said before. Preliminary conformational searches on compound **1** were run separately on the two aromatic rings (**a** and **b**, Fig. 1) with molecular mechanics (MMFF) followed by DFT geometry optimizations (B3LYP/6-31G(d)).[27] The two structures with absolute lowest energies for the two fragments were assembled together and a torsional energy scan relative to the

rotation around the chirality axis was run with the semiempirical PM3 method, which offers accurate predictions of geometries and torsional energies of biaryl compounds.[28] The scan revealed the existence of a shallow energy minimum with an almost orthogonal arrangement between the two rings. The minimum was further optimized with DFT, affording a value for $\theta_{3'\text{-}4'\text{-}10\text{-}4a}$ dihedral of 93°.

Subsequently, two starting structures were generated for compound **1** with $\theta_{3'\text{-}4'\text{-}10\text{-}4a} \approx 90°$, and full conformational searches with MMFF were run upon varying all other possible degrees of conformational freedom, involving the arrangement of the acetyl, methoxy and hydroxyl moieties. DFT optimizations of several minima thus found allowed us to isolate a limited number of structures for compound **1**. The geometry with absolute lowest energy is labeled I (see Fig. 2, left). Three other energy minima (II–IV) were obtained differing in the arrangement of the methylketone moiety at C-2′, with relative energies between +0.3–+0.8 kcal mol^{-1} from the absolute minimum; structures and relative energies are reported in the Supporting Information†. Other minima differing in the arrangement of the methoxy moieties had relative energies >2 kcal mol^{-1} and were overlooked. Incidentally, the lowest energy structure for the ND tautomer (Supporting Information†) had much higher DFT energy (+4.15 kcal mol^{-1}) than the lowest energy structure for the PQ tautomer.

CD calculations were run on the above set of structures I–IV and with ZINDO and TDDFT methods, both of which are expected to predict CD spectra of biaryls with good accuracy.[26] TDDFT calculations were run at CAM-B3LYP/SVP level. Use of a larger basis set for all geometries was impractical, however we verified on the lowest energy structure I the consistency between CAM-B3LYP/SVP and CAM-B3LYP/TZVP results (see Supporting Information†). All input structures had (a*S*) configuration of the chirality axis (positive C-4a′,C-4′,C-10,C-4a dihedral $\Theta_{4a'\text{-}4'\text{-}10\text{-}4a}$). Fig. 4a displays the CD spectra calculated on the four low-energy structures I–IV. In Fig. 4b, the experimental spectrum is compared with the weighted average of the same spectra in the most important 190–380 region. The average was evaluated weighing the calculated spectra for structures I–IV at 300 K with a Boltzmann distribution, employing DFT-computed internal energies. All the calculated spectra, and notably their average, show a positive CD couplet feature in the 210–270 nm region with crossover point around 235 nm, near to the computed absorption maximum which is between 225–230 nm. Thus, the most important feature of the experimental spectrum of (+)-rufoolivacin A (**1**) was reproduced. It is important to notice that all structures considered in the calculations gave rise to a similar positive couplet-like feature in the same region. Thus, independently of the accuracy of estimated relative populations of the various minima, a positive CD couplet would be anyway obtained by spectral averaging. The same result was obtained by employing the ZINDO method, which afforded calculated CD spectra pretty similar to TDDFT ones (shown in the Supporting Information†). ZINDO calculations were also employed to verify the impact of rotation around the chirality axis near the energy minimum having $\Theta_{4a'\text{-}4'\text{-}10\text{-}4a} \approx 90°$. Three structures were built from I with $\Theta_{4a'\text{-}4'\text{-}10\text{-}4a}$ fixed at 70°, 80° and 100° values, corresponding to PM3 energies 0.44, 0.24 and 0.17 kcal mol^{-1} above the minimum, respectively. ZINDO calculations on these structures led to CD spectra somewhat different from that calculated on I, however, in all cases, a positive couplet-like feature was observed centred around 235 nm.

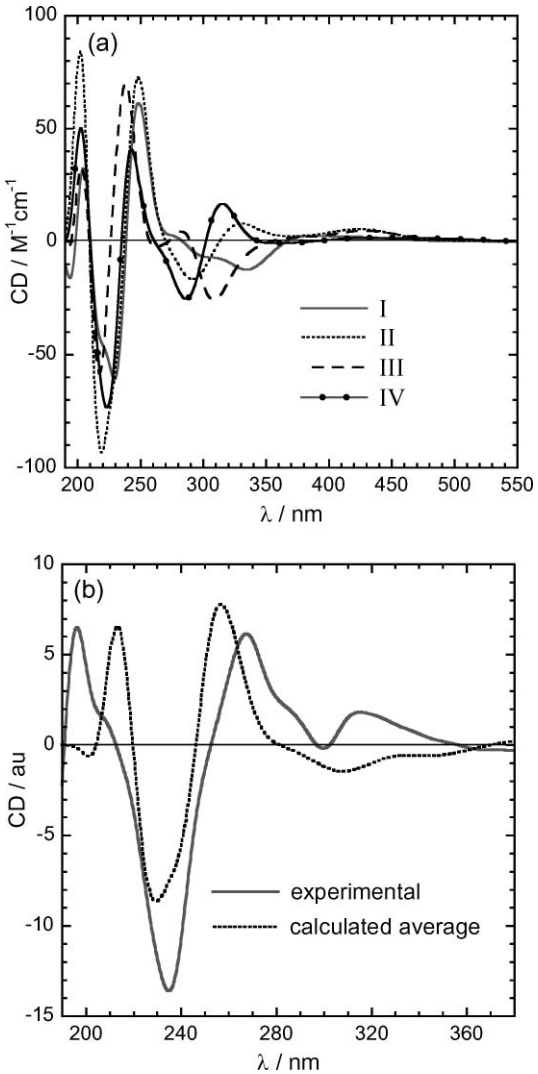

Fig. 4 (a) CD spectra calculated with CAM-B3LYP/SVP on the low-energy structures I–IV optimized with B3LYP/6-31G(d) for (a*S*)-rufoolivacin A (**1**). (b) Weighted average of the four spectra shown in (a) compared with the experimental spectrum for (+)-rufoolivacin A (**1**). Structures I–IV and relative energies are shown in the Supporting Information. A wavelength correction of +10 nm was applied to the calculated spectrum in (b).

Although the longer wavelength range of the CD spectrum of **1** is not perfectly reproduced by either TDDFT or ZINDO calculations, the consistency found in the prediction of the most prominent spectral feature makes us confident enough of the configurational assignment of rufoolivacin A as (+)-(a*S*)-**1**. Since the experimental CD spectrum of rufoolivacin B (**2**) is almost superimposable to that of **1**, its absolute configuration may also be assigned as (+)-(a*S*)-**2**. It is noteworthy that the above assignments are opposite to those obtained with a "naïf" application of the exciton chirality method, as discussed above. The apparent reason for such a discrepancy is that in the 210–270 nm region several transitions are computed, thus what appears as a CD couplet is actually the convolution of a lot of CD bands with various signs and intensities. In these conditions, a straightforward application of the exciton chirality method is clearly prone to error.

The CD spectra of rufoolivacins C and D (**3** and **4**) are shown in Fig. 3b. Although some differences emerge with respect to the CD spectra of other rufoolivacins A and B (**1** and **2**), they similarly show a distinct CD couplet in the 235–285 nm region with crossover at 260 nm. Therefore, following the same arguments as above, we tentatively assign their absolute configurations as (+)-(a*S*)-**3** and (+)-(a*S*)-**4** as well.

Fungi are well-known producers of both anthraquinones, such as 6-*O*-methylalaternin, and dihydroanthracenones such as atrochrysone, torosachrysone and 8-*O*-methyl torosachrysone. These latter ones enjoy an especially widespread distribution in toadstools belonging to the genus *Cortinarius*.[5,6,7,8] Biogenetically, monomeric dihydroanthracenones have been identified as octaketides produced through condensation, hydrolysis, decarboxylation, and enolization of acetate and/or malonate units,[7,8,9,29] suggesting that these secondary metabolites are part of a common biogenetic route. Notably, both 1,2- and 1,4-anthraquinones could arise from putative precursors dihydroanthracenones. In addition, monomeric torachrysone and its 8-*O*-methyl ether have been identified as heptaketides produced *via* condensation of acetate and/or malonate units.[8] Finally, oxidative coupling by C-10/C-4′ between dihydroanthracenone-derived anthrone (at C-10) and torachrysone monomethyl ether (at C-4′) intermediate could lead to the production of rufoolivacins (Scheme 1). Although no experimental data for enzymatic coupling of the two monomers could be obtained, it is most likely that rufoolivacins might be

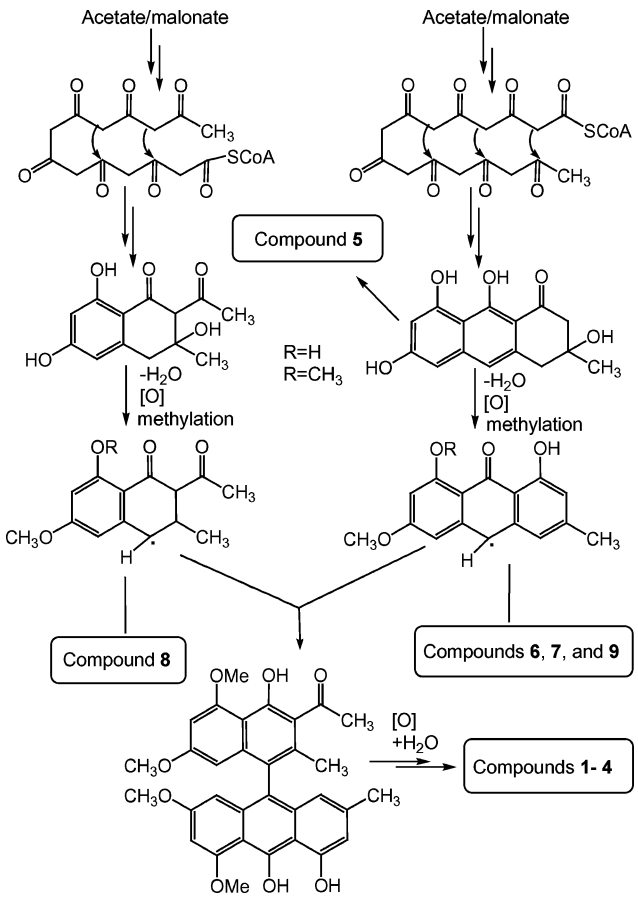

Scheme 1

Table 3 Toxicity of the pigments **1–11** with mortality rates (%)

	Toxicity										
Sample	**1**	**2**	**3**	**4**	**5**	**6**	**7**	**8**	**9**	**10**	**11**
Mortality	38.3	43.1	28.6	36.9	16.6	40.6	39.2	12.4	36.6	47.5	48.5

formed by oxidative coupling. It is noteworthy that in the present work two precursors, (3*S*)-torosachrysone-8-*O*-methyl ether (**5**) and torachrysone-8-*O*-methyl ether (**8**), were identified along with the other co-existing metabolites such as **6**, **7**, and **9**. This may further strongly support the above mentioned biosynthetic route of the polyketide pigments **1–4**. Interestingly, compound **8** was previously isolated from the seeds of *Karwinskia humboldtiana*.[2,16]

This is the first report of the concomitant occurrence of pigments of rufoolivacins **3** and **4** with coupled 1-naphthol and 1,2-anthraquinone motifs *via* a 4′,10 aryl linkage to be isolated from natural sources, to the best of our knowledge. Although naturally occurring 1,4-anthraquinones are relatively rare,[20] they are still more common than 1,2-anthraquinones. The red pigment hallachrome (7-hydroxy-8-methoxy-6-methyl-1,2-anthraquinone) was the first 1,2-anthraquinone natural product to be isolated in 1972 from the epidermal epithelial cells of the rare sea worm *Halla parthenopeia*[30] and was synthesized in 1993 for the first time by Krohn and Khanbabaee.[31] Indeed, the only other 1,2-anthraquinone natural product is sinapiquinone, a red pigment recently isolated by Gill and Milanovic from the Australasian toadstool *Cortinarius sinapicolor*.[17] In addition, compound **11** was previously obtained from an Australian *Dermocybe* toadstool.[18]

All the isolated metabolites **1–11** were tested for *in vitro* toxic activity toward brine shrimp. They were found to show weak to moderate growth inhibitory effects on brine shrimp larvae at concentrations of 10 μg ml^{-1}, as given in Table 3. The pigments **10** and **11** were found to possess moderate toxicity, with mortality rates of 47.5% and 48.5%, respectively. The results show how important the 9,10-anthraquinone moiety appears for the toxic activity of these compounds. Moreover, in the fully aromatic rufoolivacin series the *para*-quinoid rufoolivacins **1** and **2** displayed higher activity than that of the *ortho*-quinoid isomers **3** and **4**, which suggests that the presence of *para*-quinoid unit may be required for activity. Interestingly, this was in accord with antiplasmodial activity.[13]

Conclusions

In summary, four aromatic octaketide pigments rufoolivacins A (**1**), B (**2**), C (**3**) and D (**4**), members of the rare rufoolivacin class of compounds, formed *via* the 4′,10-coupled aryl linkage between 1-naphthol and 1,4- or 1,2-anthraquinone, were isolated from the fruiting bodies of a fungus, a Chinese toadstool *Cortinarius rufo-olivaceus*, together with previously isolated other polyketides (**5–11**). Their structures were deduced from NMR spectroscopic data, and the absolute axial stereochemistry of rufoolivacins **1** and **2** confirmed by CD analysis. This is the first time that the axial chirality configuration of **1** and **2** has been determined unequivocally. These metabolites were found to exert some toxic effects on brine shrimp larvae.

Experimental section

General

Melting points were determined on an XRC-1 micro-melting point apparatus and are uncorrected. The optical rotations were measured on a Perkin-Elmer polarimeter 241 polarimeter at the sodium D line. IR spectra were recorded on a Perkin-Elmer 1600 Series FT-IR spectrometer with KBr pellets, peaks are reported in cm^{-1}. UV/vis spectra were recorded on a Varian Cary 100 UV-visible spectrophotometer; peak wavelengths are reported in nm. CD spectra were recorded with a J-715 spectropolarimeter by using 0.2 mm cell on 2–2.5 mM solutions. ^{1}H NMR spectra were recorded on Varian Inova 500 (499.8 MHz), and Varian Inova 600 (600 MHz). Coupling constants (J) in Hz. Abbreviations: s = singlet, d = doublet, dd = doublet doublet, t = triplet, q = quartet, m = multiplet, br = broad. ^{13}C NMR spectra were recorded with Bruker Avance 500 (125.7 MHz), and Varian Inova 600 (150.7 MHz). Chemical shifts were measured relative to tetramethylsilane (TMS) as internal standard. Mass spectra were recorded with EI MS at 70 eV with Varian MAT 731, Varian 311A, AMD-402, high resolution with perflurokerosine as standard. ESI mass spectra were recorded on a Quattro Triple Quadrupol mass spectrometer, with a Finnigan TSQ 7000 with nano-ESI API ion source. High-resolution ESI mass spectra were measured on a Micromass LCT mass spectrometer coupled with a HP 1100 HPLC with a diode array detector.

Thin layer chromatography (TLC) and preparative TLC (PLC) were performed on Merck precoated silica gel 60 F_{254} and Merck Kieselgel 60 GF_{254} (20 g silica gel spread on 20 × 20 cm glass plates), respectively. Commercial silica gel (230–400 mesh, Merck) was used for column chromatography. Gel permeation chromatography was done on Sephadex LH-20 (Pharmacia). Visualisation was under UV light (254 or 366 nm). Fractions were monitored by TLC and spots were visualized by heating silica gel plates sprayed with 10% H_2SO_4 in ethanol. All solvents used were of analytical grade.

Fungal material

The fresh fruiting bodies of *Cortinarius rufo-olivaceus* were collected from Helan Mountain in Ningxia province, China, in the summer of 2006 and were identified by Mr Ming-Shen Bai, College of Life Sciences, University of Ningxia, Yingchuan, Ningxia. A voucher specimen is deposited in the Herbarium of University of Ningxia.

Extraction and isolation

The dried and powdered fruiting bodies (5 kg) of *Cortinarius rufo-olivaceus* were extracted five times with MeOH at room temperature. The combined organic layers were concentrated *in vacuo* to give a purple extract (187 g). The extract was partitioned successively between H_2O and petroleum ether, AcOEt, and then *n*-butanol. The AcOEt-soluble extract (6.9 g) was separated by CC on silica gel with CH_2Cl_2–MeOH (100% CH_2Cl_2, 50 : 1, 30 : 1, 20 : 1,10:1, 100% MeOH) to provide six fractions designated A–F.

Fraction B (2.72 g) was chromatographed over Sephadex LH-20 column (CH_2Cl_2–MeOH = 6 : 4) and (MeOH) successively, which provided four subfractions (Ba–d). Subfraction Bc3 was submitted to a silica gel column eluted with cyclohexane-acetone (3 : 1, 2 : 1) to afford two parts Bc3-1 and Bc3-2, the former Bc3-1 was separated by preparative TLC with CH_2Cl_2–MeOH (20 : 1), and was further purified by Sephadex LH-20 column (MeOH) to yield **1** (7.7 mg) and **3** (16.5 mg), respectively. Subfractions Bd2 obtained by a Sephadex LH-20 column (MeOH) was subjected to a Sephadex LH-20 column (acetone) to give subfractions Bd2-1 and Bd2-2. The latter Bd2-2 was separated by a silica gel column eluted with CH_2Cl_2–MeOH (40 : 1, 35 : 1) to yield **8** (11 mg) and **7** (7.7 mg), respectively.

Fraction C (1.66 g) was chromatographed over Sephadex LH-20 column (CH_2Cl_2–MeOH = 6 : 4) to obtain four subfractions (Ca–d). Subfraction Cc was passed through a Sephadex LH-20 column (MeOH) to obtain three subfractions (Cc1–3). Subfraction Cc2 was subjected to a Sephadex LH-20 column (acetone), and purified by a silica gel column eluting with CH_2Cl_2–MeOH (20 : 1) to give **10** (14.3 mg). Subfraction Cd was passed through a Sephadex LH-20 column (MeOH) to obtain three subfractions (Cd1–3). Subfraction Cd2 was submitted to a silica gel column and was eluted with cyclohexane-acetone (2 : 1, 1 : 1) to obtain two subfractions (Cd2-1, Cd2-2). The Cd2-2 was further purified by a RP-C18 silica gel column with aqueous MeOH (35%, 45%, 55%) to obtain **2** (9.4 mg) and a crude product containing **4**. Compound **4** (12.2 mg) was obtained by further purification with a Sephadex LH-20 column (MeOH).

Fraction D (4.28 g) was chromatographed over a Sephadex LH-20 column with CH_2Cl_2–MeOH (6 : 4) to provide three subfractions (Da–c). Subfractions Da2 obtained by a Sephadex LH-20 column (MeOH) was purified by a Sephadex LH-20 column (acetone), and followed by a silica gel column eluting with CH_2Cl_2–MeOH (20 : 1) to afford **11** (9.2 mg). Subfraction Db was passed through a Sephadex LH-20 column (MeOH) to secure two subfractions (Db1 and Db2). Subfraction Db1 yielded **5** (8.2 mg) and **6** (4.3 mg) by purification with a Sephadex LH-20 column (acetone). Compound **9** (6.2 mg) was repeatedly purified from subfraction Db2 by Sephadex LH-20 column (acetone, and MeOH).

Rufoolivacin A (1). Red amorphous powder. m.p. 260–264 °C; $[\alpha]_D^{22}$ = +240 (c = 0.12, MeOH); UV/Vis (MeOH): $\lambda(\varepsilon)$ = 203 (7762), 238 (12303), 283 (sh, 5370), 324 (2512), 475 (sh, 1259), 512 (1995), 535 nm (sh, 1660 L mol^{-1} cm^{-1}); CD (MeOH, $c \approx 2.5 \times 10^{-3}$): λ, nm (ellipticity, mdeg) = 234 (–13.5), 266 (6.0), 299 (–0.1), 314 (1.8), 444 (–0.6), 499 (0.5). IR (KBr): ν_{max} = 3390, 2937, 1652, 1604, 1450, 1368, 1202, 1162, 1109, 1054, 823 cm^{-1}; HR-MS (ESI): m/z calcd. for $C_{32}H_{29}O_9$: 557.1807; 557.1806 $[M+H]^+$; ^{1}H- and ^{13}C-NMR spectroscopic data, see Table 1.

Rufoolivacin B (2). Red amorphous powder. m.p. 342–346 °C; $[\alpha]_D^{22}$ = +88 (c = 0.12, MeOH); UV/Vis (MeOH): $\lambda(\varepsilon)$ = 207 (sh, 19953), 237 (27542), 286 (sh, 14791), 325 (7413), 478 (sh, 4266), 512 (5888), 535 nm (sh, 5129 L mol^{-1} cm^{-1}); CD (MeOH, $c \approx 2.5 \times 10^{-3}$): λ, nm (ellipticity, mdeg) = 229 (–13.5), 266 (4.4), 300 (–0.5), 317 (1.7), 438 (–0.8), 503 (0.6). IR (KBr): ν_{max} = 3422, 2928, 1658, 1599, 1457, 1374, 1202, 1162, 1107, 1055, 829 cm^{-1}; HR-MS (ESI): m/z calcd. for $C_{32}H_{29}O_{10}$: 573.1755; found: 573.1748 $[M+H]^+$; ^{1}H- and ^{13}C-NMR spectroscopic data, see Table 1.

Rufoolivacin C (3). Red amorphous powder. m.p. 304–308 °C; $[\alpha]_D^{22}$ = +320 (c = 0.10, MeOH); UV/Vis (MeOH): λ (ε) = 214

(sh, 18197), 242 (23988), 283 (sh, 7762), 333 (5495), 507 nm (2455 L mol^{-1} cm^{-1}); CD (MeOH, $c \approx 2.0 \times 10^{-3}$): λ, nm (ellipticity, mdeg) = 214 (6.3), 230 (−5.5), 250 (−6.3), 268 (+5.0), 297 (−2.9), 363 (−1.2). IR (KBr): ν_{max} = 3392, 2931, 1650, 1601, 1457, 1371, 1202, 1162, 1110, 1052, 830 cm^{-1}; HR-MS (ESI): *m/z* calcd. for $C_{32}H_{29}O_9$: 557.1805; found: 557.1804 $[M+H]^+$; ^{1}H- and ^{13}C-NMR spectroscopic data, see Table 2.

Rufoolivacin D (4). Red amorphous powder. M.p. 356–360 °C; $[\alpha]_D^{22}$ = +110 (*c* = 0.10, MeOH); UV/Vis (MeOH): λ (ε) = 202 (sh, 13490), 239 (20893), 245 (sh, 20417), 335 (3802), 509 nm (1514 L mol^{-1} cm^{-1}); CD (MeOH, $c = 2.6 \times 10^{-3}$): λ, nm (ellipticity, mdeg) = 211 (2.9), 228 (−4.3), 250 (−7.3), 268 (4.13), 293 (−1.4), 367 (−0.9) nm. IR (KBr): ν_{max} = 3434, 2930, 1621,1601, 1458, 1370, 1202, 1161, 1114, 1052, 829 cm^{-1}; HR-MS (ESI): *m/z* calcd. for $C_{32}H_{29}O_{10}$: 573.1755; found: 573.1754 $[M+H]^+$; ^{1}H- and ^{13}C-NMR spectroscopic data, see Table 2.

Brine shrimp bioassay

The brine shrimp toxicity was assayed by small modified microtiter-plate method using brine shrimp *Artemia salina* as a test organism. Briefly, approximately 30 nuclei larvae hatched from eggs of *A. salina* in 0.2 ml of artificial sea water were incubated with a sample (5 µl in DMSO solution) in a deep-well microtiter plate at room temperature. After 24 h, the dead larvae were determined by counting the number of dead animals in each well under microscope. To each test row, a blind sample was accompanied by adding DMSO only. The mortality rate was calculated using the formula: $M = [(A - B - N)/(G - N)] \times 100$

M = percent of dead larvae after 24 h; A = number of dead larvae after 24 h; B = average number of dead larvae in the blind samples after 24 h; N = number of dead larvae before starting the test; G = number of selected larvae for test.

The animal experiments were performed in compliance with the relevant laws and institutional guidelines of the University of Göttingen, that approved the experiments and the guidelines and legislation that were followed.

Computational section

MMFF conformational searches, PM3 torsional energy scans and DFT geometry optimizations were run with Spartan'06 (Wavefunction, Inc., Irvine, CA) using default parameters and convergence criteria. TDDFT and ZINDO calculations were run with Gaussian'03 and Gaussian'09 (Gaussian, Inc., Wallingford CT),[32] including respectively 36 and 50 excited states. CAM-B3LYP/SVP combination was used in TDDFT calculations, and, in one case, CAM-B3LYP/TZVP.[33] CD spectra were generated using dipole-length rotational strengths and applying a Gaussian band-shape with 1500–2000 cm^{-1} half-height width. For CAM-B3LYP/TZVP calculations, the difference with dipole-velocity values for the most intense CD bands was negligible (<15%).

Acknowledgements

We would like to acknowledge funding support from the National Natural Science Foundation of China (Grant No. 30370019, 30670221, and 30770237), the Program for Changjiang Scholars and Innovative Research Team in University (IRT0749), the Scientific Research Foundation for the Returned Overseas Chinese Scholars, State Education Ministry of China, as well as by the Program for New Century Excellent Talents in University (NCET-05-0852). A program supported by the National Financial Aid for Studying Abroad (2007103088) (J.-C.Q.) is also gratefully acknowledged. The authors would also like to thank Prof. H. Laatsch and F. Lissy for technical assistance and H. Frauendorf and R. Machinek, in the Laboratory of Institution for Organic and Biomolecular Chemistry, University of Göttingen, Germany, for the MS and NMR measurements. Finally, thanks are also due to Prof. Xuan Tian, in the Key State Laboratory of Functional Organic Molecules, University of Lanzhou, China) for recording CD and UV spectra.

References

1 (*a*) J. Schümann and C. Hertweck, *J. Biotechnol.*, 2006, **124**, 690–703; (*b*) R. Thomas, *ChemBioChem*, 2001, **2**, 612–627; (*c*) T. J. Simpson, *Nat. Prod. Rep.*, 1991, **8**, 573–602; (*d*) J. M. Crawford, T. P. Korman, J. W. Labonte, A. L. Vagstad, E. A. Hill, O. Kamari-Bidkorpeh, S. C. Tsai and C. A. Townsend, *Nature*, 2009, **461**, 1139–43; (*e*) B. J. Rawlings, *Nat. Prod. Rep.*, 1997, **14**, 523–556.
2 D. L. Dreyer, I. Arai, C. D. Bachman, W. R. Anderson, Jr., R. G. Smith and G. D. Daves, Jr, *J. Am. Chem. Soc.*, 1975, **97**, 4985–4990.
3 (*a*) G. Alemayehu, A. Hailu and B. M. Abegaz, *Phytochemistry*, 1996, **42**, 1423–1425; (*b*) G. Alemayehu and B. M. Abegaz, *Phytochemistry*, 1996, **41**, 919–921; (*c*) H. Anke, I. Kolthoum, H. Zfhner and H. Laatsch, *Arch. Microbiol.*, 1980, **126**, 223–230; (*d*) A. Yagi, N. Okamura, H. Haraguchi, T. Abo and K. Hashimoto, *Phytochemistry*, 1993, **33**, 87–91; (*e*) H. Haraguchi, T. Abo, A. Fukuda, N. Okamura and A. Yagi, *Phytochemistry*, 1996, **43**, 989–992; (*f*) R. L. Edwards and H. J. Lockett, *J. Chem. Soc., Perkin Trans. 1*, 1976, 2149–2155; (*g*) M. Gill and P. M. Morgan, *Arkivoc*, 2001, 145–156; (*h*) K. Beattie, C. Elsworth, M. Gill, N. M. Milanovic, D. Prima-Putra and E. Raudies, *Phytochemistry*, 2004, **65**, 1033–1038; (*i*) M. A. Archard, M. Gill and R. J. Strauch, *Phytochemistry*, 1985, **24**, 2755–2758.
4 (*a*) M. S. Buchanan, M. Gill and J. Yu, *J. Chem. Soc., Perkin Trans. 1*, 1997, 919–926; (*b*) M. Gill, A. Gimenez, A. G. Jhingran, N. M. Milanovic and A. R. Palfreyman, *J. Chem. Soc., Perkin Trans. 1*, 1998, 3431–3436; (*c*) M. Gill, *Nat. Prod. Rep.*, 1994, **11**, 67–90; (*d*) M. Gill, *Nat. Prod. Rep.*, 1996, **13**, 513–528; (*e*) M. Gill, *Nat. Prod. Rep.*, 1999, **16**, 301–317.
5 M. Gill, *Nat. Prod. Rep.*, 2003, **20**, 615–639.
6 C. Elsworth, M. Gill, A. Gimenez, N. M. Milanovic and E. Raudies, *J. Chem. Soc., Perkin Trans. 1*, 1999, 119–126.
7 M. Gill, *Aust. J. Chem.*, 2001, **54**, 721–734.
8 M. Gill and W. Steglich, *Progr. Chem. Org. Nat. Prod.*, 1987, **51**, 1–317.
9 M. Müller, K. Lamottke, W. Steglich, S. Busemann, M. Reichert, G. Bringmann and P. Spiteller, *Eur. J. Org. Chem.*, 2004, 4850–4855.
10 L.-F. Zan, T. Bau, H.-Y. Bao and Y. Li, *J. Fungal Res.*, 2008, **2**, 101–105.
11 L.-F. Zan, T. Bau, H.-Y. Bao and Y. Li, *Mycosystema*, 2008, **27**, 284–288.
12 J.-M. Gao, *Curr. Org. Chem.*, 2006, **10**, 849–871.
13 G. Francois, T. Steenackers, L. A. Assi, W. Steglich, K. Lamottke, J. Holenz and G. Bringmann, *Parasitol. Res.*, 1999, **85**, 582–588.
14 (*a*) M. S. Buchanan, M. Gill, P. Millar, S. Phonh-Axa, E. Raudies and J. Yu, *J. Chem. Soc., Perkin Trans. 1*, 1999, 795–802; (*b*) M. Gill, A. Gimenez, A. G. Jhingran and A. R. Palfreyman, *Tetrahedron Lett.*, 1990, **31**, 1203–1206.
15 B. J. Ma, Y. Ruan and J. K. Liu, *Nat. Prod. Res. Dev.*, 2008, **20**, 63–65.
16 S. Shibata, E. Morishita, M. Kaneda, Y. Kimura, M. Takido and S. Takahashi, *Chem. Pharm. Bull.*, 1969, **17**, 454–457.
17 M. Gill and N. M. Milanovic, *Aust. J. Chem.*, 1999, **52**, 1035–1040.
18 M. Gill, E. Raudies and J. Yu, *Aust. J. Chem.*, 1999, **52**, 989–992.
19 (*a*) T. W. Doyle, D. E. Nettleton, R. E. Grulich, D. M. Balitz, D. L. Johnson and A. L. Vulcano, *J. Am. Chem. Soc.*, 1979, **101**, 7041–7049; (*b*) M. Gill and A. Gimenez, *Tetrahedron Lett.*, 1990, **31**, 3505–3508.
20 R. H. Thomson, in *'Naturally Occurring Quinones'*, 3rd Edn, (Chapman & Hall: London, 1987).
21 G. Alemayehu, A. Hailu and B. M. Abegaz, *Phytochemistry*, 1996, **42**, 1423–1425.

22 (*a*) N. Harada, K. Nakanishi, *Circular Dichroic Spectroscopy - Exciton Coupling in Organic Stereochemistry*, Oxford University Press: Oxford, 1983; (*b*) N. Berova, L. Di Bari and G. Pescitelli, *Chem. Soc. Rev.*, 2007, **36**, 914–931.
23 K. Arai, Y. Aoki and Y. Yamamoto, *Chem. Pharm. Bull.*, 1989, **37**, 621–625.
24 (*a*) S. F. Mason, R. H. Seal and D. R. Roberts, *Tetrahedron*, 1974, **30**, 1671–1682; (*b*) L. Di Bari, G. Pescitelli and P. Salvadori, *J. Am. Chem. Soc.*, 1999, **121**, 7998–8004.
25 (*a*) S. F. Mason, *J. Chem. Soc., Chem. Commun.*, 1973, 239–241; (*b*) G. Gottarelli, G. Proni, G. P. Spada, D. Fabbri, S. Gladiali and C. Rosini, *J. Org. Chem.*, 1996, **61**, 2013–2019.
26 (*a*) T. D. Crawford, *Theor. Chem. Acc.*, 2006, **115**, 227–245; (*b*) C. Diedrich and S. Grimme, *J. Phys. Chem. A*, 2003, **107**, 2524–2539; (*c*) G. Bringmann, T. A. M. Gulder, M. Reichert and T. Gulder, *Chirality*, 2008, **20**, 628–642; (*d*) J. Autschbach, *Chirality*, 2008, **21**, S116–S152; (*e*) G. Pescitelli, T. Kurtán, U. Flörke and K. Krohn, *Chirality*, 2009, **21**, S181–S201.
27 C. J. Cramer, *Essentials of Computational Chemistry*, 2nd ed.; Wiley-VCH: Chichester, 2004.
28 S. Yao, C.-P. Tang, Y. Ye, T. Kurtán, A. Kiss-Szikszai, S. Antus, G. Pescitelli, P. Salvadori and K. Krohn, *Tetrahedron: Asymmetry*, 2008, **19**, 2007–2014 and references therein.
29 (*a*) A. Stoessl, C. H. Unwin and J. B. Stothers, *Can. J. Chem.*, 1983, **61**, 372–377; (*b*) A. Stoessl, C. H. Unwin and J. B. Stothers, *Tetrahedron Lett.*, 1979, **20**, 2481–2484.
30 G. Prota, M. D'Agostino and G. Misuraca, *J. Chem. Soc., Perkin Trans. 1*, 1972, 1614–1616.
31 K. Krohn and K. Khanbabaee, *Liebigs Ann. Chem.*, 1993, 905–909.
32 (*a*) M. J. Frisch, G. W. Trucks, H. B. Schlegel, G. E. Scuseria, M. A. Robb, J. R. Cheeseman, J. A. Montgomery, Jr., T. Vreven, K. N. Kudin, J. C. Burant, J. M. Millam, S. S. Iyengar, J. Tomasi, V. Barone, B. Mennucci, M. Cossi, G. Scalmani, N. Rega, G. A. Petersson, H. Nakatsuji, M. Hada, M. Ehara, K. Toyota, R. Fukuda, J. Hasegawa, M. Ishida, T. Nakajima, Y. Honda, O. Kitao, H. Nakai, M. Klene, X. Li, J. E. Knox, H. P. Hratchian, J. B. Cross, V. Bakken, C. Adamo, J. Jaramillo, R. Gomperts, R. E. Stratmann, O. Yazyev, A. J. Austin, R. Cammi, C. Pomelli, J. Ochterski, P. Y. Ayala, K. Morokuma, G. A. Voth, P. Salvador, J. J. Dannenberg, V. G. Zakrzewski, S. Dapprich, A. D. Daniels, M. C. Strain, O. Farkas, D. K. Malick, A. D. Rabuck, K. Raghavachari, J. B. Foresman, J. V. Ortiz, Q. Cui, A. G. Baboul, S. Clifford, J. Cioslowski, B. B. Stefanov, G. Liu, A. Liashenko, P. Piskorz, I. Komaromi, R. L. Martin, D. J. Fox, T. Keith, M. A. Al-Laham, C. Y. Peng, A. Nanayakkara, M. Challacombe, P. M. W. Gill, B. G. Johnson, W. Chen, M. W. Wong, C. Gonzalez and J. A. Pople, *GAUSSIAN 03 (Revision D.01)*, Gaussian, Inc., Wallingford, CT, 2004; (*b*) M. J. Frisch, G. W. Trucks, H. B. Schlegel, G. E. Scuseria, M. A. Robb, J. R. Cheeseman, G. Scalmani, V. Barone, B. Mennucci, G. A. Petersson, H. Nakatsuji, M. Caricato, X. Li, H. P. Hratchian, A. F. Izmaylov, J. Bloino, G. Zheng, J. L. Sonnenberg, M. Hada, M. Ehara, K. Toyota, R. Fukuda, J. Hasegawa, M. Ishida, T. Nakajima, Y. Honda, O. Kitao, H. Nakai, T. Vreven, J. A. Montgomery, Jr., J. E. Peralta, F. Ogliaro, M. Bearpark, J. J. Heyd, E. Brothers, K. N. Kudin, V. N. Staroverov, R. Kobayashi, J. Normand, K. Raghavachari, A. Rendell, J. C. Burant, S. S. Iyengar, J. Tomasi, M. Cossi, N. Rega, J. M. Millam, M. Klene, J. E. Knox, J. B. Cross, V. Bakken, C. Adamo, J. Jaramillo, R. Gomperts, R. E. Stratmann, O. Yazyev, A. J. Austin, R. Cammi, C. Pomelli, J. Ochterski, R. L. Martin, K. Morokuma, V. G. Zakrzewski, G. A. Voth, P. Salvador, J. J. Dannenberg, S. Dapprich, A. D. Daniels, O. Farkas, J. B. Foresman, J. V. Ortiz, J. Cioslowski and D. J. Fox, *GAUSSIAN 09 (Revision A.2)*, Gaussian, Inc., Wallingford, CT, 2009.
33 See Gaussian'09 documentation at www.gaussian.com/g_tech/g_ur/g09help.htm for reference on basis sets and DFT functionals.